The Astrophysical Journal, 622:28–38, 2005 March 20
© 2005. The American Astronomical Society. All rights reserved. Printed in U.S.A.

GENERALIZED CHAPLYGIN GAS MODELS TESTED WITH TYPE Ia SUPERNOVAE

Marek Biesiada
Department of Astrophysics and Cosmology, University of Silesia, Uniwersytecka 4, 40-007 Katowice, Poland; mb@imp.sosnowiec.pl

and

Włodzimierz Godłowski and Marek Szydłowski
Astronomical Observatory, Jagiellonian University, Orla 171, Krakow, Poland; godlows@oa.uj.edu.pl, szydlo@oa.uj.edu.pl
Received 2004 April 14; accepted 2004 December 5

ABSTRACT

The generalized Chaplygin gas (GCG), with the equation of state $p = -A/\rho^{\alpha}$, was recently proposed as a candidate for dark energy in the universe. In this paper we confront the GCG with Type Ia supernova (SN Ia) data using available samples. Specifically, we have tested the GCG cosmology in three different classes of models with (1) $\Omega_m = 0.3$ and $\Omega_{\rm Ch} = 0.7$, (2) $\Omega_m = 0.05$ and $\Omega_{\rm Ch} = 0.95$, and (3) $\Omega_m = 0$ and $\Omega_{\rm Ch} = 1$, as well as a model without prior assumptions on Ω_m. The best-fit models are obtained by minimizing the χ^2 function. We supplement our analysis with confidence intervals in the (A_0, α)-plane by marginalizing the probability density functions (pdf's) over the remaining parameters assuming uniform priors. We have also derived one-dimensional pdf's for $\Omega_{\rm Ch}$ obtained from joint marginalization over α and A_0. The maximum value of such a pdf provides the most probable value of $\Omega_{\rm Ch}$ within the full class of GCG models. The general conclusion is that SN Ia data give support to the Chaplygin gas (with $\alpha = 1$). However, a noticeable preference for A_0-values close to 1 means that the α dependence becomes insignificant. This is reflected in one-dimensional pdf's for α that turned out to be flat, meaning that the power of the present supernova data to discriminate between various GCG models (differing by α) is weak. Extending our analysis by relaxing the prior assumption of the flatness of the universe leads to the result that even though the best-fit values of Ω_k are formally nonzero, they are still close to the flat case. Our results show clearly that in GCG cosmology, distant (i.e., $z > 1$) supernovae should be brighter than in the ΛCDM model. Therefore, one can expect that future supernova experiments (e.g., *SNAP*) having access to higher redshifts will eventually resolve the issue of whether the dark energy content of the universe could be described as a Chaplygin gas. Moreover, it would be possible to differentiate between models with various values of the α-parameter and/or discriminate between GCG, Cardassian, and ΛCDM models. This discriminative power of the forthcoming mission has been demonstrated on simulated *SNAP* data.

Subject headings: cosmology: theory — distance scale — supernovae: general

1. INTRODUCTION

For a couple of years, two independent observational programs, the high-redshift supernova surveys (Riess et al. 1998; Perlmutter et al. 1999) and cosmic microwave background radiation (CMBR) small-scale anisotropy measurements (de Bernardis et al. 2000; Benoit et al. 2003; Hinshaw et al. 2003), have brought a new picture of the universe at large. While interpreted within the FRW models, results of these programs suggest that our universe is flat (as inferred from the location of acoustic peaks in the CMBR power spectrum) and currently accelerates its expansion (as inferred from the Type Ia supernova [SN Ia] Hubble diagram). Combined with independent knowledge about the amount of baryons and cold dark matter (CDM), estimated to be $\Omega_m = 0.3$ (Turner 2002), it follows that about an $\Omega_X = 0.7$ fraction of the critical density $\rho_{\rm cr} = 3c^2H_0^2/8\pi G$ should be contained in a mysterious component called "dark energy." The most obvious candidate for this smooth component permeating the universe is the cosmological constant Λ, representing the energy of the vacuum. Well-known fine-tuning problems led many people to seek beyond the Λ framework, and the concept of the quintessence had been conceived. Usually, the quintessence is described in a phenomenological manner, as a scalar field with an appropriate potential (Ratra & Peebles 1988; Caldwell et al. 1998; Frieman et al. 1995). It turns out, however, that the quintessence program also suffers from its own fine-tuning problems (Kolda & Lyth 1999).

In 1904 the Russian physicist Chaplygin introduced the exotic equation of state $p = -A/\rho$ to describe an adiabatic aerodynamic process (Chaplygin 1904). The attractiveness of this equation of state in the context of dark energy models comes mainly from the fact that it gives a unification of both dark energy (postulated in cosmology to explain the current acceleration of the universe) and clustered dark matter, which is postulated in astrophysics to explain the flat rotation curves of spiral galaxies. It is interesting that the Chaplygin gas can be derived from the quintessence Lagrangian for the scalar field ϕ with some potential and also from the Born-Infeld form of the Lagrangian (Kamenshchik et al. 2001). The Chaplygin equation of state has some interesting connections with string theory (Ogawa 2000), and it admits interpretation in the framework of brane cosmologies (Jackiw 2000). Recently, this Chaplygin gas (Kamenshchik et al. 2001; Fabris et al. 2002; Szydłowski & Czaja 2004) was proposed as a challenge to the above-mentioned candidates for dark energy. Currently, its generalizations admitting the equation of state $p = -A/\rho^{\alpha}$, where $0 \leq \alpha \leq 1$, have been proposed (Bento et al. 2002; Carturan & Finelli 2003).

In this paper we confront the generalized Chaplygin gas (GCG) with SN Ia data. At this point, our choice of GCG cosmologies deserves some justification. There are two approaches in the literature. The first one is phenomenological, i.e., having no preferred theory of dark energy responsible for acceleration of the universe, in which one characterizes dark energy as a cosmic fluid with an equation of state $p_X = w\rho_X$, where $w \geq -1$

(see, e.g., Chiba et al. 1998; Turner & White 1997, and an immense amount of literature that appeared thereafter). Because, as already mentioned above, a strain of ideas about dark energy is associated with an evolving scalar, there are good reasons to expect that the cosmic equation of state could be time dependent, i.e., $w = w(t) = w(z)$ (e.g., Weller & Albrecht 2001; Maor et al. 2001, and many others thereafter). This approach seems attractive from the perspective of analyzing observational data such as supernova surveys, and indeed this approach was taken while first analyzing the data (Riess et al. 1998, 2004; Perlmutter et al. 1999; Knop et al. 2003). However, even though such analysis places constraints on *any* potential theory that might explain the dark energy phenomenon, ultimately one always ends up at testing a *specific* theory. Along this line, there appeared attempts to reconstruct the scalar field potential, assuming that the scalar field was responsible for dark energy (e.g., Alam et al. 2003 and references therein). Our approach goes along this philosophy but instead is devoted to the GCG, which has recently been considered as a candidate for a unified dark matter and dark energy component (i.e., responsible for both clustering and accelerated expansion; Makler et al. 2003).

The cosmological models with the GCG also have many special features that make them attractive. In the standard cosmological model, one can clearly distinguish the epochs of radiation domination followed by (ordinary) matter domination (with decelerated expansion). As mentioned above, supernova data suggest that the epoch of decelerated expansion ended and switched to an accelerated epoch, dominated by dark energy. The GCG models describe smoothly the transition from the decelerated to accelerated epochs. They represent the simplest deformation of concordance ΛCDM (Gorini et al. 2003). Moreover, they propose a new unified macroscopic (phenomenological) description of both dark energy and dark matter. This places them in a distinguished position from the point of view of the Occam's razor principle. It should also be noted that the GCG model allows us to explain the currently observed acceleration of the universe without the cosmological constant and/or modification of Einstein's equations.

If one takes seriously the given dark energy scenario (necessary to explain cosmic acceleration), one should also consider the behavior of perturbations in such a universe. In the framework of quintessence models with the barytropic equation of state (i.e., $p = w\rho$ and $w = \text{const}$), one faces the problem of instabilities on short scales. This appears because the speed of sound squared (equal here to w) is negative (and constant). Calculation of the sound speed in the GCG model (see below) reveals its nonbarytropic nature. The perturbations in GCG models are stable on short scales even in an accelerating phase (Carturan & Finelli 2003). Moreover, they behave like dust perturbations when Chaplygin gas is in the dust regime.

Another motivation for studying GCG models comes from theoretical physics, specifically from attempts to describe the dark energy in terms of the Lagrangian for a tachyonic field (Garousi 2000; Sen 2002). Of course, it would be nice to have a description of dark energy in terms of the nonquintessence Lagrangian, as it describes the nature of dark energy, while the cosmological constant is the only phenomenological and effective description. One should also note that the GCG equation of state arises in modern physics in the context of brane models (Bordemann & Hoppe 1993; Kamenshchik et al. 2001; Randall & Sundrum 1999), where the GCG manifests itself as an effect of the immersion of our universe in multidimensional bulk space.

GCG models have been intensively studied in the literature, and in particular they have been tested against supernova data (Makler et al. 2003; Avelino et al. 2003; Colistete et al. 2004), lensing statistics (Dev et al. 2003; Silva & Bertolami 2003), CMBR measurements (Bento et al. 2003a, 2003b; Carturan & Finelli 2003; Amendola et al. 2003), the age-redshift relation (Alcaniz et al. 2003), X-ray luminosities of galaxy clusters (Cunha et al. 2004), and the large-scale structure considerations (Bean & Doré 2003; Multamäki et al. 2004; Bilic et al. 2004). Perspectives on distinguishing between GCG, brane-world scenarios, and quintessence in forthcoming gravity wave experiments have been discussed in Biesiada (2003). Although the results are, in general, mutually consistent, there was no strong convergence to unique values of the A_0 and α parameters characterizing the Chaplygin gas equation of state.

Makler et al. (2003) considered the FRW model filled completely with GCG and concluded that the whole class of such models is consistent with current SN Ia data, although the value of $\alpha = 0.4$ is favored. This result has been confirmed by our analysis (class 3 models). However, when the existing knowledge about the baryonic matter content of the universe was incorporated into the study, our results were different from those of Makler et al. (2003), who found that $\alpha = 0.15$ was preferred (assuming $\Omega_m = 0.04$, which is very close to our assumption for class 2 models).

As noted by Bean & Doré (2003), GCG models have an inherent degeneracy with cosmological constant models as far as background evolution is concerned, and therefore they have a good fit with SN Ia data. These degeneracies disappear at the level of evolution of perturbations, and hence confrontation with the CMBR spectrum would be decisive. Using available data on the positions of CMBR peaks measured by BOOMERANG (de Bernardis et al. 2000), ARCHEOPS (Benoit et al. 2003), and *WMAP* (Hinshaw et al. 2003), Bento et al. (2003a, 2003b) obtained the following constraints: $0.81 \leq A_0 \leq 0.85$ and $0.2 \leq \alpha \leq 0.6$ at the 68% confidence level in the model representative of our class 2 (i.e., with $\Omega_m = 0.05$ assumed). Another estimation of the parameter α was done by Amendola et al. (2003) with *WMAP* data. They obtained $0 \leq \alpha < 0.2$ at the 95% confidence level.

Using the angular size statistics for extragalactic sources combined with SN Ia data, it was found in Alcaniz & Lima (2005) that in the $\Omega_m = 0.3$ and $\Omega_{\rm Ch} = 0.7$ scenario, the best-fit values of the model parameters are $A_0 = 0.83$ and $\alpha = 1$. A recent paper by Bertolami et al. (2004), in which GCG models have been analyzed against Tonry et al. (2003) supernova data relaxing the prior assumption on flatness, suggests, surprisingly, as the authors admit, the preference of $\alpha > 1$.

2. COSMOLOGICAL MODEL

The Einstein equations for the FRW model with hydrodynamic energy-momentum tensor $T_{\mu\nu} = (\rho + p)u_\mu u_\nu - p g_{\mu\nu}$ read

$$\left(\frac{\dot{a}}{a}\right)^2 = \frac{8\pi G\rho}{3} - \frac{k}{a^2(t)}, \tag{1}$$

$$\frac{\ddot{a}(t)}{a} = -\frac{4\pi G}{3}(\rho + 3p). \tag{2}$$

Let us assume that the matter content of the universe consists of pressureless gas with energy density ρ_m, representing baryonic matter plus CDM, and the GCG with the equation of state

$$p_{\rm Ch} = -\frac{A}{\rho_{\rm Ch}^{\alpha}}, \tag{3}$$

representing the dark energy responsible for the acceleration of the universe. If one further makes an assumption that these two components do not interact, then the energy conservation equation,

$$\dot{\rho} + 3H(p + \rho) = 0, \tag{4}$$

where $H = \dot{a}/a$ is the Hubble function, can be integrated separately for matter and Chaplygin gas, leading to the well-known result $\rho_m = \rho_{m,0}a^{-3}$ and (see also Bento et al. 2002; Carturan & Finelli 2003)

$$\rho_{\rm Ch} = \left(A + \frac{B}{a^{3(1+\alpha)}}\right)^{1/(1+\alpha)}. \tag{5}$$

The physical interpretation of the (so far arbitrary) constants A and B is as follows. Adopting the usual convention that the current value of the scale factor a_0 is equal to 1, one can see that $\rho_{\rm Ch,0} = (A + B)^{1/(1+\alpha)}$ represents the current energy density of the Chaplygin gas. Calculating the adiabatic speed of sound squared for the Chaplygin gas,

$$c_s^2 = \frac{\partial p_{\rm Ch}}{\partial \rho_{\rm Ch}} = \frac{\alpha A}{\rho^{1+\alpha}} = \frac{\alpha A}{A + B/a^{3(1+\alpha)}},$$

it is easy to confirm that the current value of c_s^2 is $c_{s,0}^2 = \alpha A/(A + B)$. Hence the constants A and B can be expressed as combinations of quantities having well-defined physical meaning.

Our further task is to confront the Chaplygin gas model with SN Ia data, and for this purpose we have to calculate the luminosity distance in our model,

$$d_L(z) = (1+z)\frac{c}{H_0}\frac{1}{\sqrt{|\Omega_k|}}\mathcal{F}\left(H_0\sqrt{|\Omega_k|}\int_0^z \frac{dz'}{H(z')}\right), \tag{6}$$

where $\Omega_k = -k/H_0^2$ and

$$\mathcal{F}(x) = \begin{cases} \sinh x & \text{for } k < 0, \\ x & \text{for } k = 0, \\ \sin x & \text{for } k > 0. \end{cases} \tag{7}$$

The Friedman equation (eq. [1]) can be rearranged to the form giving explicitly the Hubble function $H(z) = \dot{a}/a$,

$$H(z)^2 = H_0^2\Big\{\Omega_m(1+z)^3 + \Omega_{\rm Ch}\Big[A_0 + (1-A_0)(1+z)^{3(1+\alpha)}\Big]^{1/(1+\alpha)} + \Omega_k(1+z)^2\Big\}, \tag{8}$$

where the quantities Ω_i ($i = m$, Ch, and k) represent the fractions of the critical density currently contained in energy densities of the respective components, and $\Omega_m + \Omega_{\rm Ch} + \Omega_k = 1$. For the transparency of further formulae, we have also denoted $A_0 = A/(A + B)$.

Finally, the luminosity distance reads

$$d_L(z) = (1+z)\frac{c}{H_0}\frac{1}{\sqrt{|\Omega_k|}}\mathcal{F}\left(\sqrt{|\Omega_k|}\int_0^z \Big\{\Omega_m(1+z')^3 + \Omega_{\rm Ch}\Big[A_0 + (1-A_0)(1+z')^{3(1+\alpha)}\Big]^{1/(1+\alpha)} + \Omega_k(1+z')^2\Big\}^{-1/2} dz'\right). \tag{9}$$

Formula (9) is the most general one in the framework of FRW cosmology with GCG. Please note that this model proposes a unified macroscopic (phenomenological) description of both dark energy and dark matter.

In this paper we mostly use the version restricted to a flat model, $k = 0$ (the exception is when we relax the flat prior), since the evidence for this case is very strong in the light of current CMBR data. Therefore, while talking about model testing, we actually mean the estimation of the α and A_0 parameters for the best-fit flat FRW cosmological model filled with GCG.

To proceed with fitting the SN Ia data, we need the magnitude-redshift relation,

$$m(z, \mathcal{M}, \Omega_m, \Omega_{\rm Ch}; A_0, \alpha) = \mathcal{M} + 5\log_{10}D_L(z, \Omega_m, \Omega_{\rm Ch}; A_0, \alpha), \tag{10}$$

where

$$D_L(z, \Omega_m, \Omega_{\rm Ch}; A_0, \alpha) = H_0 d_L(z, H_0, \Omega_m, \Omega_{\rm Ch}; A_0, \alpha)$$

is the luminosity distance with H_0 factored out, so that marginalization over the intercept

$$\mathcal{M} = M - 5\log_{10}H_0 + 25 \tag{11}$$

actually leads to joint marginalization over H_0 and M (M being the absolute magnitude of the SN Ia).

Then we can obtain the best-fit model minimizing the χ^2 function,

$$\chi^2 = \sum_i \frac{\left(m_i^{\rm Ch} - m_i^{\rm obs}\right)^2}{\sigma_i^2},$$

where the sum is over the SN Ia sample and σ_i denote the (full) statistical error of magnitude determination. This is illustrated by Figures 2 and 3, below, which show residuals (with respect to the Einstein–de Sitter model) and χ^2 levels in the (A_0, α)-plane. One of the advantages of residual plots is that the intercept of the m-z curve gets canceled. The assumption that the intercept is the same for different cosmological models is legitimate, since $\mathcal{M}$ is actually determined from the low-redshift part of the Hubble diagram, which should be linear in all realistic cosmologies.

The best-fit values alone are not relevant if not supplemented with the confidence levels for the parameters. Therefore, we performed the estimation of model parameters using the minimization procedure, based on the likelihood function. We assumed that the supernova measurements came with uncorrelated Gaussian errors, and in this case the likelihood function $\mathcal{L}$ could be determined from the χ^2 statistic by $\mathcal{L} \propto \exp(-\chi^2/2)$ (Riess et al. 1998; Perlmutter et al. 1999).

Therefore, we supplement our analysis with confidence intervals in the (A_0, α)-plane by calculating the marginal probability density functions (pdf's),

$$\mathcal{P}(A_0, \alpha) \propto \int \exp\left[-\chi^2(\Omega_m, \Omega_{\rm Ch}, A_0, \alpha, \mathcal{M})/2\right] d\mathcal{M},$$

with Ω_m and $\Omega_{\rm Ch}$ fixed ($\Omega_m = 0.0$, 0.05, and 0.3), and

$$\mathcal{P}(A_0, \alpha) \propto \int \exp\left[-\chi^2(\Omega_m, \Omega_{\rm Ch}, A_0, \alpha, \mathcal{M})/2\right] d\Omega_m,$$

with $\mathcal{M}$ fixed ($\mathcal{M} = -3.39$; proportionality sign means equal up to the normalization constant). In order to complete the picture, we have also derived one-dimensional pdf's for $\Omega_{\rm Ch}$ obtained from joint marginalization over α and A_0. The maximum value of such a pdf informs us about the most probable value of $\Omega_{\rm Ch}$ (supported by supernova data) within the full class of GCG models.

3. FITS TO A_0 AND α PARAMETERS

3.1. *Samples Used*

Supernova surveys (published data) already have a 5 year long history. Beginning with the first published samples, other data sets have been produced either by correcting original samples for systematic errors or by supplementing them with new supernovae (or both). It is not our intention here to suggest a distinguished role for any one of these data sets. Therefore, in our analysis we decided to use a collection of samples from all existing supernova data.

The latest data were compiled by Riess et al. (2004), and since they became available, they have been used by many researchers as a standard data set. However, for the sake of comparison and illustration we also analyzed three earlier samples of supernovae. This seems to be useful, because, as pointed out in the literature, studies performed on different SN Ia samples often gave different results (see, e.g., Godłowski et al. 2004; Choudhury & Padmanabhan 2005).

Samples from the original Perlmutter et al. (1999) data chosen for the analysis comprise the full sample reported by Perlmutter (sample A) and a subsample after excluding two outliers differing the most from the average light curve and two outliers claimed likely to be reddened (sample C). Although the outliers often suggest statistical inhomogeneity of the data (and some hints suggesting the necessity of removing them from sample A exist), there is always a danger that removal of outliers is to some extent subjective. Therefore, we retained the full sample A in our analysis.

Then Knop et al. (2003) reexamined the Perlmutter et al. (1999) data with host-galaxy extinction correctly assessed. From the Perlmutter sample they chose only those supernovae that were spectroscopically safely identified as SNe Ia and had reasonable color measurements. They also included 11 new high-redshift supernovae and a well-known sample with low-redshift supernovae. In Knop et al. (2003), a few subsamples have been distinguished. We considered two of them. The first is a subset of 58 supernovae with corrected extinction (Knop subsample 6; hereafter K6), and the second is a subset of 54 low-extinction supernovae (Knop subsample 3; hereafter K3). Samples C and K3 are similarly constructed as containing only low-extinction supernovae. The advantage of the Knop sample is that the discussion by Knop et al. (2003) of extinction correction was very careful, and as a result, their sample has extinction correctly applied.

Another sample was presented by Tonry et al. (2003), who collected a large number of supernova data published by different authors and added eight new high-redshift SNe Ia. This sample of 230 SNe Ia was recalibrated with a consistent zero point. Wherever possible, the extinction estimates and distance fitting were recalculated. Unfortunately, we were unable to do so for the full sample (for details, see Table 8 in Tonry et al. 2003). This sample was further improved by Barris et al. (2004), who added 23 high-redshift supernovae, including 15 at $z \geq 0.7$, thus doubling the published record of objects at these redshifts. We have chosen two Tonry-Barris subsamples. First, we considered the full Tonry-Barris sample of 253 low-extinction SNe Ia (hereafter sample TBI). Because the Tonry sample has a lot of outliers, especially at low redshifts, we decided to analyze the sample of 193 SNe Ia in which all low-redshift ($z < 0.01$) and high-extinction supernovae were excluded (hereafter sample TBII).

Tonry et al. (2003) and Barris et al. (2004) presented the redshifts and luminosity distances for their supernova sample. Therefore, equations (10) and (11) should be modified appropriately to (Williams et al. 2003)

$$m - M = 5 \log_{10}(D_L)_{\rm Tonry} - 5 \log_{10} 65 + 25, \tag{12}$$

$$\mathcal{M} = -5 \log_{10} H_0 + 25. \tag{13}$$

For the Hubble constant $H_0 = 65$ km s^{-1} Mpc^{-1}, one gets $\mathcal{M} = 15.935$.

Recently, Riess et al. (2004) significantly improved the former Riess sample. They discovered 16 new SNe Ia. It should be noted that six of these objects have $z > 1.25$ (out of total number of seven objects with such high redshifts). Moreover, they compiled a set of previously observed SNe Ia, relying on large, published samples whenever possible to reduce systematic errors from differences in calibrations. With this enriched sample, it became possible to test our prediction that distant supernovae in GCG cosmology should be brighter than in the ΛCDM model (see discussion in § 3.3).

The full Riess et al. (2004) sample contains 186 SNe Ia ("Silver" sample). On the basis of quality of the spectroscopic and photometric record for individual supernovae, they also selected a more restricted "Gold" sample of 157 supernovae. We have separately analyzed the ΛCDM model for supernovae with $z < 1$ and for all SNe Ia belonging to the Gold sample.

3.2. *Cosmological Models Tested*

On these samples, we have tested GCG cosmology in three different classes of models, with (1) $\Omega_m = 0.3$ and $\Omega_{\rm Ch} = 0.7$, (2) $\Omega_m = 0.05$ and $\Omega_{\rm Ch} = 0.95$, and (3) $\Omega_m = 0$ and $\Omega_{\rm Ch} = 1$. We started with a fixed value of $\mathcal{M} = -3.39$ and modified this assumption accordingly while analyzing different samples.

The first class was chosen as representative of the standard knowledge of Ω_m (baryonic plus dark matter in galactic halos; Peebles & Ratra 2003) with Chaplygin gas responsible for the missing part of the closure density (the dark energy). In the second class, we have incorporated (at the level of Ω_m) the prior knowledge about the baryonic content of the universe (as inferred from big bang nucleosynthesis [BBN] considerations). Hence this class is representative of the models in which Chaplygin gas is allowed to clump and is responsible both for dark matter in halos as well as its diffuse part (dark energy). The third class is a kind of toy model: the FRW universe filled completely with Chaplygin gas. We have considered it mainly in order to see how sensitive the SN Ia test is with respect to parameters identifying

TABLE 1
RESULTS OF GCG MODELS FROM MINIMUM χ^2

Sample	Ω_m	$\Omega_{\rm Ch}$	A_0	α	$\mathcal{M}$	χ^2
A	0.00	1.00	0.77	1.00	−3.39	95.4
	0.00	1.00	0.77	1.00	−3.39	95.4
	0.05	0.95	0.80	1.00	−3.39	95.4
	0.30	0.70	0.96	1.00	−3.39	95.8
C	0.00	1.00	0.80	1.00	−3.44	52.9
	0.00	1.00	0.80	1.00	−3.44	52.9
	0.05	0.95	0.83	1.00	−3.44	53.0
	0.30	0.70	0.99	1.00	−3.42	53.3
K6	0.00	1.00	0.81	1.00	−3.52	55.3
	0.00	1.00	0.81	1.00	−3.52	55.3
	0.05	0.95	0.84	1.00	−3.52	55.4
	0.30	0.70	1.00	1.00	−3.51	55.9
K3	0.00	1.00	0.85	1.00	−3.48	60.4
	0.00	1.00	0.85	1.00	−3.48	60.4
	0.05	0.95	0.87	1.00	−3.47	60.4
	0.30	0.70	1.00	1.00	−3.44	61.4
TBI	0.00	1.00	0.79	1.00	15.895	273.9
	0.00	1.00	0.79	1.00	15.895	273.8
	0.05	0.95	0.82	1.00	15.895	274.0
	0.30	0.70	0.97	1.00	15.915	275.8
TBII	0.00	1.00	0.78	1.00	15.915	186.5
	0.00	1.00	0.78	1.00	15.915	186.5
	0.05	0.95	0.81	1.00	15.915	186.6
	0.30	0.70	0.97	1.00	15.925	188.4
Silver	0.00	1.00	0.82	1.00	15.945	229.4
	0.00	1.00	0.82	1.00	15.945	229.4
	0.05	0.95	0.85	1.00	15.945	229.6
	0.30	0.70	0.99	1.00	15.965	232.3
Gold	0.00	1.00	0.81	1.00	15.945	173.7
	0.00	1.00	0.81	1.00	15.945	173.7
	0.05	0.95	0.84	1.00	15.945	173.8
	0.30	0.70	0.99	1.00	15.965	175.6

NOTES.—Results of statistical analysis of the GCG model (with marginalization over $\mathcal{M}$) performed on analyzed samples of SNe Ia (A, C, K6, K3, TBI, TBII, Silver, and Gold) as a minimum χ^2 best fit. First rows for each sample refer to no prior on Ω_m. The same analysis was repeated with fixed priors $\Omega_m = 0.0$, $\Omega_m = 0.05$, and $\Omega_m = 0.3$.

the cosmological model. Finally, we analyzed the data without any prior assumption about Ω_m.

3.3. *Results*

The results (best fits) of two fitting procedures performed on different samples and with different prior assumptions concerning the cosmological models are presented in Tables 1 and 2. Table 1 refers to the χ^2 method, whereas in Table 2 the results from marginalized pdf's are displayed. In both cases we obtained different values of $\mathcal{M}$ for each analyzed sample. This point deserves a comment.

From a purely statistical point of view, fitting $\mathcal{M}$ for each sample separately is quite obvious. However, if we recall the physical meaning of $\mathcal{M}$ (see eq. [11]), we see that if we knew the intrinsic luminosities of SNe Ia and the Hubble constant, then $\mathcal{M}$ would be a definite number. Hence it is tempting to use a fixed value of $\mathcal{M}$ calibrated on a certain reference sample for each analysis. Preliminary analysis performed on the Perlmutter et al. (1999) samples indicated that parameter estimates, especially for α, were strongly dependent on the choice of $\mathcal{M}$. As could be expected, fixing $\mathcal{M}$ produced discrepancies between subsamples (e.g., between A and C), and fitting $\mathcal{M}$ for each sample significantly improved the consistency.

For example, in the first class of models the best fit (with a fixed value of $\mathcal{M} = -3.39$) from sample A is ($\alpha = 1$, $A_0 = 0.96$) at $\chi^2 = 95.8$. Sample C gives a best fit of ($\alpha = 0.95$, $A_0 = 0.95$) at $\chi^2 = 53.6$. In the second class, sample A gives a best fit of ($\alpha = 1, A_0 = 0.80$) at $\chi^2 = 95.4$, whereas sample C gives the best fit ($\alpha = 0.51, A_0 = 0.73$) at $\chi^2 = 53.7$. Finally, in the third class sample A again gives the best fit of ($\alpha = 1$, $A_0 = 0.77$) at $\chi^2 = 95.4$, whereas sample C gives the best fit ($\alpha = 0.42$, $A_0 = 0.69$) at $\chi^2 = 53.7$.

However, the fitting procedure for sample C prefers $\mathcal{M} = -3.44$ instead of $\mathcal{M} = -3.39$, as for sample A. If one takes this value, the results for sample C will change respectively, and then for the first class $A_0 = 1$ (at $\chi^2 = 53.5$), which means (see eq. [8]) that α can be arbitrary, and the problem is effectively equivalent to the model with the cosmological constant. Analogously, for the second class $A_0 = 0.83$ and $\alpha = 1$ (at $\chi^2 = 52.9$), while for the third class $A_0 = 0.80$ and $\alpha = 1$ (at $\chi^2 = 52.9$). This indicates clearly that model parameters, especially α, strongly depend on the choice of $\mathcal{M}$.

The same thing happened if we analyzed the data without any prior assumption about Ω_m and if the marginal pdf's were used to derive the best fits. Therefore, we additionally analyzed our samples marginalized over $\mathcal{M}$ and reported the appropriate results.

From the above analysis, we concluded that the Ω_m and A_0 parameters derived from samples A and C are similar. For Ω_m fixed, A_0 increases with increasing Ω_m. The estimates of the

TABLE 2

GCG Model Parameter Values from Probability Density Functions

Sample	Ω_m	$\Omega_{\rm Ch}$	A_0	α	$\mathcal{M}$
A	$0.17^{+0.08}_{-0.17}$	$0.83^{+0.17}_{-0.08}$	$0.83^{+0.14}_{-0.09}$	$-0.0^{+0.67}$	$-3.36^{+0.05}_{-0.05}$
	0.00	1.00	$0.73^{+0.08}_{-0.10}$	$1.0_{-0.63}$	$-3.38^{+0.05}_{-0.05}$
	0.05	0.95	$0.76^{+0.08}_{-0.09}$	$1.0_{-0.66}$	$-3.38^{+0.05}_{-0.05}$
	0.30	0.70	$0.96^{+0.04}_{-0.09}$	$0.0^{+0.65}$	$-3.36^{+0.04}_{-0.03}$
C	$0.15^{+0.08}_{-0.15}$	$0.85^{+0.15}_{-0.08}$	$0.86^{+0.13}_{-0.10}$	$0.0^{+0.66}$	$-3.41^{+0.05}_{-0.05}$
	0.00	1.00	$0.76^{+0.08}_{-0.10}$	$0.49^{+0.36}_{-0.35}$	$-3.43^{+0.06}_{-0.05}$
	0.05	0.95	$0.79^{+0.08}_{-0.11}$	$0.11^{+0.57}_{-0.11}$	$-3.43^{+0.06}_{-0.05}$
	0.30	0.70	$0.99^{+0.01}_{-0.11}$	$0.0^{+0.64}$	$-3.39^{+0.04}_{-0.04}$
K6	$0.10^{+0.11}_{-0.10}$	$0.90^{+0.10}_{-0.11}$	$0.88^{+0.12}_{-0.08}$	$-0.0^{+0.66}$	$-3.51^{+0.03}_{-0.03}$
	0.00	1.00	$0.78^{+0.07}_{-0.09}$	$0.71^{+0.29}_{-0.40}$	$-3.52^{+0.04}_{-0.03}$
	0.05	0.95	$0.81^{+0.08}_{-0.09}$	$0.06^{+0.61}_{-0.06}$	$-3.52^{+0.04}_{-0.03}$
	0.30	0.70	$1.00_{-0.10}$	$0.0^{+0.64}$	$-3.49^{+0.02}_{-0.03}$
K3	$0.11^{+0.07}_{-0.11}$	$0.89^{+0.11}_{-0.07}$	$0.88^{+0.11}_{-0.05}$	$0.0^{+0.66}$	$-3.45^{+0.03}_{-0.04}$
	0.00	1.00	$0.80^{+0.06}_{-0.06}$	$0.30^{+0.39}_{-0.30}$	$-3.47^{+0.05}_{-0.04}$
	0.05	0.95	$0.84^{+0.05}_{-0.07}$	$0.0^{+0.67}$	$-3.47^{+0.05}_{-0.05}$
	0.30	0.70	$1.00_{-0.06}$	$0.0^{+0.63}$	$-3.42^{+0.03}_{-0.03}$
TBI	$0.00^{+0.21}$	$1.00_{-0.21}$	$0.81^{+0.12}_{-0.07}$	$1.0_{-0.60}$	$15.905^{+0.02}_{-0.02}$
	0.00	1.00	$0.75^{+0.04}_{-0.05}$	$1.0_{-0.54}$	$15.905^{+0.02}_{-0.02}$
	0.05	0.95	$0.78^{+0.04}_{-0.06}$	$1.0_{-0.55}$	$15.915^{+0.02}_{-0.02}$
	0.30	0.70	$0.96^{+0.04}_{-0.04}$	$0.0^{+0.67}$	$15.915^{+0.02}_{-0.02}$
TBII	$0.00^{+0.21}$	$1.00_{-0.21}$	$0.81^{+0.12}_{-0.07}$	$1.0_{-0.62}$	$15.925^{+0.02}_{-0.02}$
	0.00	1.00	$0.75^{+0.04}_{-0.06}$	$1.0_{-0.54}$	$15.915^{+0.03}_{-0.02}$
	0.05	0.95	$0.78^{+0.04}_{-0.06}$	$1.0_{-0.54}$	$15.925^{+0.03}_{-0.02}$
	0.30	0.70	$0.96^{+0.04}_{-0.04}$	$0.0^{+0.67}$	$15.935^{+0.03}_{-0.02}$
Silver	$0.00^{+0.18}$	$1.00_{-0.18}$	$0.84^{+0.09}_{-0.06}$	$1.0_{-0.59}$	$15.945^{+0.02}_{-0.02}$
	0.00	1.00	$0.79^{+0.03}_{-0.05}$	$1.0_{-0.52}$	$15.955^{+0.02}_{-0.03}$
	0.05	0.95	$0.81^{+0.04}_{-0.04}$	$1.0_{-0.54}$	$15.955^{+0.02}_{-0.02}$
	0.30	0.70	$0.99^{+0.01}_{-0.03}$	$0.0^{+0.64}$	$15.965^{+0.03}_{-0.02}$
Gold	$0.00^{+0.20}$	$1.00_{-0.20}$	$0.83^{+0.11}_{-0.07}$	$1.0_{-0.64}$	$15.955^{+0.03}_{-0.03}$
	0.00	1.00	$0.77^{+0.04}_{-0.05}$	$1.0_{-0.58}$	$15.955^{+0.02}_{-0.03}$
	0.05	0.95	$0.80^{+0.04}_{-0.05}$	$1.0_{-0.59}$	$15.955^{+0.02}_{-0.03}$
	0.30	0.70	$0.99^{+0.01}_{-0.04}$	$0.0^{+0.64}$	$15.965^{+0.02}_{-0.02}$

Notes.—GCG model parameter values obtained from the marginal pdf's calculated on Perlmutter, Knop, Tonry-Barris, and Riess samples. First rows for each sample refer to no prior on Ω_m. The same analysis was repeated with fixed priors $\Omega_m = 0.0$, $\Omega_m = 0.05$, and $\Omega_m = 0.3$.

α-parameter are different for each of the two above-mentioned samples, but unfortunately, errors are large. Discrepancy between the best-fit procedure and minimization procedure (based on the likelihood function) increases with the number of parameters fitted. The minimization procedure seems to be more appropriate in the context of our problem. We repeated our analysis without prior assumptions on Ω_m. The density distributions (one-dimensional pdf) for model parameters obtained by marginalization over the remaining parameters of the model are presented in Figure 1.

One can see from Table 1 that using the Knop et al. (2003) samples did not influence the conclusions in a significant way. However, the errors of parameter estimation decreased noticeably (see Table 2). The minimization procedure prefers (especially for

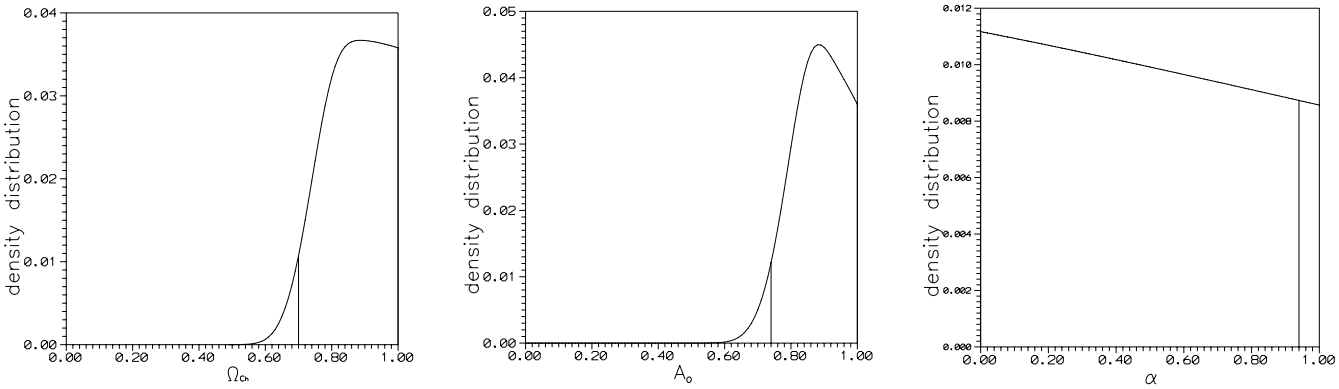


Fig. 1.—Density distributions (one-dimensional pdf's) for $\Omega_{\rm Ch}$, A_0, and α obtained from sample K3 by marginalization over the remaining parameters of the model. We obtain the limits $\Omega_{\rm Ch} > 0.70$, $A_0 > 0.74$, and $\alpha < 0.94$ at the confidence level of 95.4%.

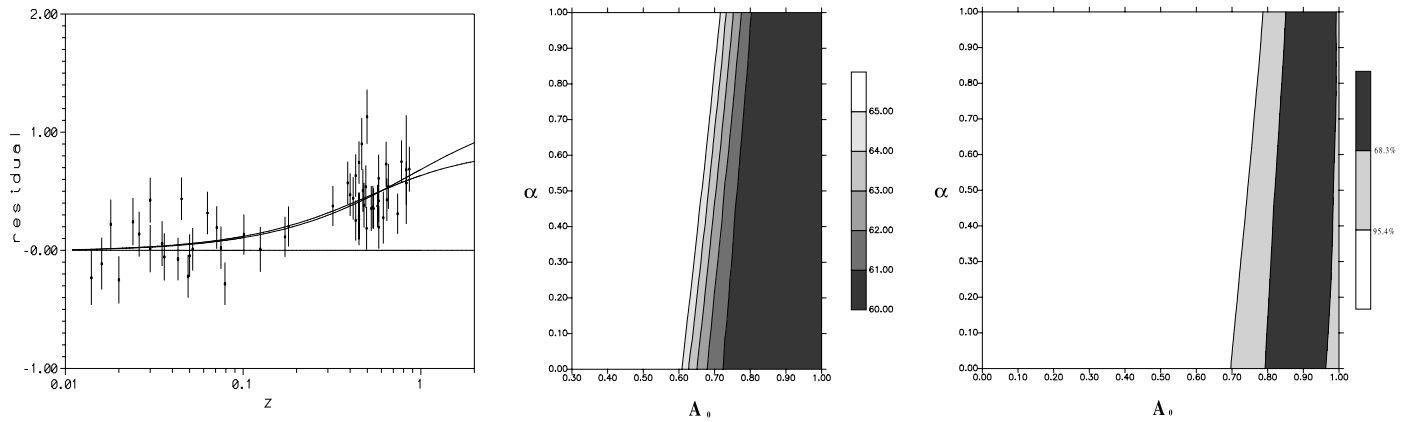


FIG. 2.—Results from sample K3. *Left*: Residuals (in mag) between the Einstein–de Sitter model (*zero line*), the flat ΛCDM model (*upper curve*), and the best-fit GCG model without prior assumptions on Ω_m (*middle curve*). *Center*: Levels of constant χ^2 on the plane (A_0, α) for the GCG model. *Right*: Confidence levels on the plane (A_0, α) for the GCG model, marginalized over $\mathcal{M}$ and Ω_m.

sample K3) α to be close to zero. The exception is the model with $\Omega_m = 0$, where $\alpha = 0.3$ and $\alpha = 0.71$ are obtained for samples K3 and K6, respectively.

The above-mentioned results for the Knop et al. (2003) sample K3 and Riess et al. (2004) Gold sample are illustrated in Figures 2 and 3. Three types of figures are displayed. First, we present residual plots of redshift-magnitude relations between the Einstein–de Sitter model (represented by the zero line), the best-fit GCG model without prior assumptions on Ω_m (*middle curve*), and the flat ΛCDM model with $\Lambda = 0.75$ and $\Omega_m = 0.25$ (*upper curve*). One can observe that systematic deviation between the ΛCDM model and the GCG model gets larger at higher redshifts. The GCG model predicts that high-redshift supernovae should be brighter than predicted with the ΛCDM model. Then, levels of constant χ^2 on the (A_0, α)-plane for the GCG model without prior assumptions on Ω_m, marginalized over $\mathcal{M}$, are presented in the center panels. Finally, the right panels show the confidence levels on the (A_0, α)-plane.

One should note that as a best fit, we obtain $\Omega_m = 0$, $\Omega_{\rm Ch} = 1$, $A_0 = 0.85$, and $\alpha = 1$, i.e., the results are the same as for a toy model with Chaplygin gas only ($\Omega_{\rm Ch} = 1$). Formally, we could have analyzed models with $\alpha > 1$. However, because of the large error in the estimation of the α-parameter, it does not seem reasonable to analyze such a possibility with current supernova data.

The results of a similar analysis obtained with the Tonry-Barris sample are similar to those obtained with previous samples. For example, the TBII sample gives the best fit, $\Omega_m = 0$, $\Omega_{\rm Ch} = 1$, $A_0 = 0.78$, and $\alpha = 1$, i.e., nearly the same as in the case of the K3 sample.

Joint marginalization over parameters gives the following results: $\Omega_{\rm Ch} = 1.00$ (hence $\Omega_m = 0.0$), with the limit $\Omega_{\rm Ch} \geq 0.79$ at the confidence level of 68.3% and $\Omega_{\rm Ch} \geq 0.67$ at the confidence level of 95.4%, and ($\alpha = 1.0$, $A_0 = 0.81$), with the limit $\alpha \in (0.40, 1)$ and $A_0 \in (0.74, 0.93)$ at the confidence level of 68.3% and $\alpha \in (0.06, 1)$ and $A_0 \in (0.70, 1.00)$ at the confidence level of 95.4%.

However, with the minimization procedure we find an important difference between results obtained with the Tonry-Barris sample and those obtained with Perlmutter C and Knop samples. The minimization procedure (except the model with fixed $\Omega_m = 0.3$) performed on Tonry-Barris data gives $\alpha = 1$. This is significantly different from the result obtained for the Perlmutter and Knop samples, where the minimization procedure preferred small values of the α-parameter. In addition, the Tonry-Barris sample preferred a value of $\Omega_m = 0$, while the Perlmutter and Knop samples suggested that Ω_m is close to zero, which indicates that the baryonic component is small, in agreement with BBN.

The new Riess sample leads to results that are similar to those obtained with the Tonry-Barris sample. However, the errors in the estimation of the parameters are lower. For the Gold sample, joint marginalization over the parameters gives the following

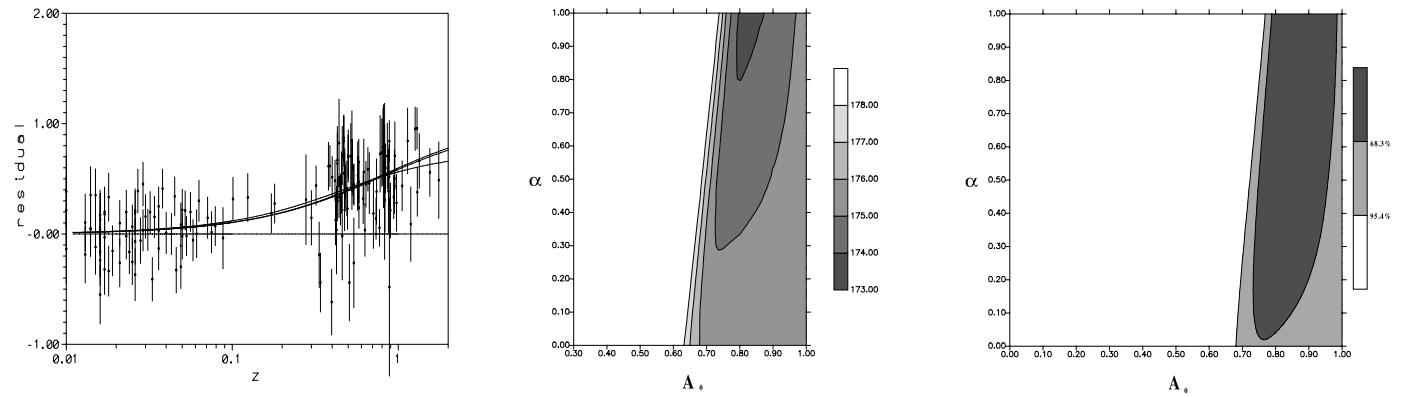


FIG. 3.—Results from Gold sample. *Left*: Residuals (in mag) between the Einstein–de Sitter model (*zero line*), flat ΛCDM model (*two upper curves*: for SN Ia with $z < 1$ [*highest curve*] and for all SNe Ia belonging to the sample [*next-highest curve*]), and the best-fit GCG model without any prior assumptions on Ω_m (*middle curve*). *Center*: Levels of constant χ^2 on the plane (A_0, α) for the GCG model. *Right*: Confidence levels on the plane (A_0, α) for the GCG model, marginalized over $\mathcal{M}$ and Ω_m.

TABLE 3

GCG Models with Flat Prior Relaxed from Minimum χ^2

Sample	Ω_k	Ω_m	$\Omega_{\rm Ch}$	A_0	α	$\mathcal{M}$	χ^2
K3.....	−0.19	0.00	1.19	0.82	1.00	−3.48	60.3
	−0.25	0.00	1.25	0.82	1.00	−3.49	60.3
	−0.28	0.05	1.23	0.84	1.00	−3.49	60.3
	−0.48	0.30	1.18	0.93	0.97	−3.49	60.3
Gold.....	−0.12	0.00	1.12	0.80	0.99	15.945	173.4
	−0.13	0.00	1.13	0.81	1.00	15.935	173.4
	−0.17	0.05	1.12	0.83	1.00	15.935	173.4
	−0.31	0.30	1.01	0.94	1.00	15.955	173.6

Notes.—Results of statistical analysis of GCG models with the flat prior relaxed and with marginalization over $\mathcal{M}$ performed on Knop sample K3 and the Gold sample as a minimum χ^2 best fit. First rows refer to no prior on Ω_m. The same analysis was repeated with fixed $\Omega_m = 0.0$, $\Omega_m = 0.05$, and $\Omega_m = 0.3$.

results: $\Omega_{\rm Ch} = 1.00$ (hence $\Omega_m = 0.0$), with the limit $\Omega_{\rm Ch} \geq 0.80$ at the confidence level of 68.3% and $\Omega_{\rm Ch} \geq 0.69$ at the confidence level of 95.4%, and ($\alpha = 1.0$, $A_0 = 0.83$), with the limit $\alpha \in (0.36, 1)$ and $A_0 \in (0.76, 0.94)$ at the confidence level of 68.3% and $\alpha \in (0.05, 1)$ and $A_0 \in (0.72, 1.00)$ at the confidence level of 95.4%.

Figure 3 shows the results for the Gold sample and is again organized into three panels. As one can see from the left panel of Figure 3, the differences between the results obtained in both cases are small (however, the result obtained with the full Gold sample leads to the prediction of brighter distant supernovae than in the case with $z < 1$ SNe Ia). Note that in the plot of residuals we have two curves corresponding to the flat ΛCDM model: one for SN Ia with $z < 1$ (*highest curve*) and one for all SNe Ia belonging to the sample (*next-highest curve*). The best-fit GCG model (without prior assumptions on Ω_m) corresponds to the middle curve. One can see that most distant supernovae are actually brighter than predicted in the ΛCDM model. This is in agreement with the prediction of the GCG cosmology. It is also apparent from Figure 3 that confidence levels on the (A_0, α)-plane (for the Gold sample) are comparable at the 95.4% confidence level with the results obtained on the the Knop sample. However, the preferred values of α are different.

3.4. *Flat Prior Relaxed*

We extended our analysis by adding a curvature term to the original GCG model. Then in equation (9) we must take into account the Ω_k term. For statistical analysis we restricted the values of the Ω_m parameter to the interval [0, 1], $\Omega_{\rm Ch}$ to the interval [0, 2], and Ω_k was obtained from the constraint $\Omega_m + \Omega_{\rm Ch} + \Omega_k = 1$. However, the cases $\Omega_k < -1$ were excluded from the analysis. The results are presented in Tables 3 and 4, displaying best fits to cosmological parameters obtained from χ^2 and marginal pdf's, respectively. Density distribution functions (one-dimensional pdf's) for model parameters obtained by marginalization over the remaining parameters of the model are presented in Figure 4.

In the model without prior assumptions on Ω_m, we obtain with the Knop sample $\Omega_k = -0.19$ as a best fit, while the maximum-likelihood method prefers $\Omega_k = -0.60$. However, for models with priors on Ω_m or $\Omega_{\rm Ch}$ (see § 3.2), the maximum-likelihood method prefers a universe much "closer" to the flat one. Specifically, for the toy model with Chaplygin gas only, one gets $\Omega_k = 0.10$ and $\Omega_k = 0.05$ for the model with baryonic content only, i.e., $\Omega_m = 0.05$. We should emphasize that even though we allowed $\Omega_k \neq 0$, the preferred model of the universe is nearly a flat one, which is in agreement with CMBR data. This is an advantage of our GCG model as compared with the ΛCDM model, where in Riess et al. (1998) and Perlmutter et al. (1999) a high negative value of Ω_k was obtained as a best fit, although a zero value of Ω_k was statistically admissible. In order to find the curvature of the universe, they additionally used data from CMBR and extragalactic astronomy.

Our main result here is that the preference of the nearly flat universe is confirmed with the new Riess et al. (2004) sample. In the model without a prior assumption on Ω_m we obtain $\Omega_k = -0.12$ as a best fit with the Gold sample, while maximum-likelihood method prefers $\Omega_k = -0.32$, i.e., the Gold sample gives an even "more flat" universe than the Knop sample. The models with priors on Ω_m also give very similar results when we

TABLE 4

GCG Models with Flat Prior Relaxed from Probability Density Functions

Sample	Ω_k	Ω_m	$\Omega_{\rm Ch}$	A_0	α	$\mathcal{M}$
K3.....	$-0.60^{+0.38}_{-0.38}$	$0.00^{+0.29}$	$1.26^{+0.25}_{-0.39}$	$0.89^{+0.11}_{-0.07}$	$0.0^{+0.64}$	$-3.46^{+0.05}_{-0.05}$
	$0.10^{+0.37}_{-0.60}$	0.00	$0.90^{+0.59}_{-0.37}$	$0.76^{+0.10}_{-0.07}$	$0.0^{+0.66}$	$-3.46^{+0.04}_{-0.05}$
	$0.05^{+0.31}_{-0.58}$	0.05	$0.90^{+0.58}_{-0.31}$	$0.78^{+0.10}_{-0.06}$	$0.0^{+0.66}$	$-3.47^{+0.05}_{-0.05}$
	$-0.35^{+0.17}_{-0.40}$	0.30	$1.05^{+0.41}_{-0.17}$	$0.88^{+0.09}_{-0.05}$	$0.0^{+0.63}$	$-3.47^{+0.04}_{-0.04}$
Gold.....	$-0.32^{+0.25}_{-0.25}$	$0.00^{+0.28}$	$1.06^{+0.24}_{-0.22}$	$0.82^{+0.13}_{-0.05}$	$0.0^{+0.64}$	$15.945^{+0.03}_{-0.03}$
	$-0.19^{+0.29}_{-0.28}$	0.00	$1.19^{+0.28}_{-0.29}$	$0.76^{+0.03}_{-0.05}$	$0.85^{+0.15}_{-0.52}$	$15.945^{+0.02}_{-0.03}$
	$-0.20^{+0.28}_{-0.29}$	0.05	$1.15^{+0.29}_{-0.28}$	$0.78^{+0.05}_{-0.06}$	$0.54^{+0.36}_{-0.32}$	$15.945^{+0.02}_{-0.03}$
	$-0.30^{+0.21}_{-0.23}$	0.30	$1.00^{+0.23}_{-0.21}$	$0.91^{+0.04}_{-0.05}$	$0.00^{+0.60}$	$15.945^{+0.02}_{-0.03}$

Notes.—Results of statistical analysis of GCG models with the flat prior relaxed and with marginalization over $\mathcal{M}$ performed on Knop sample K3 and the Gold sample. Model parameter values are obtained from the marginal pdf's. First rows refer to no prior on Ω_m. The same analysis was repeated with fixed $\Omega_m = 0.0$, $\Omega_m = 0.05$, and $\Omega_m = 0.3$.

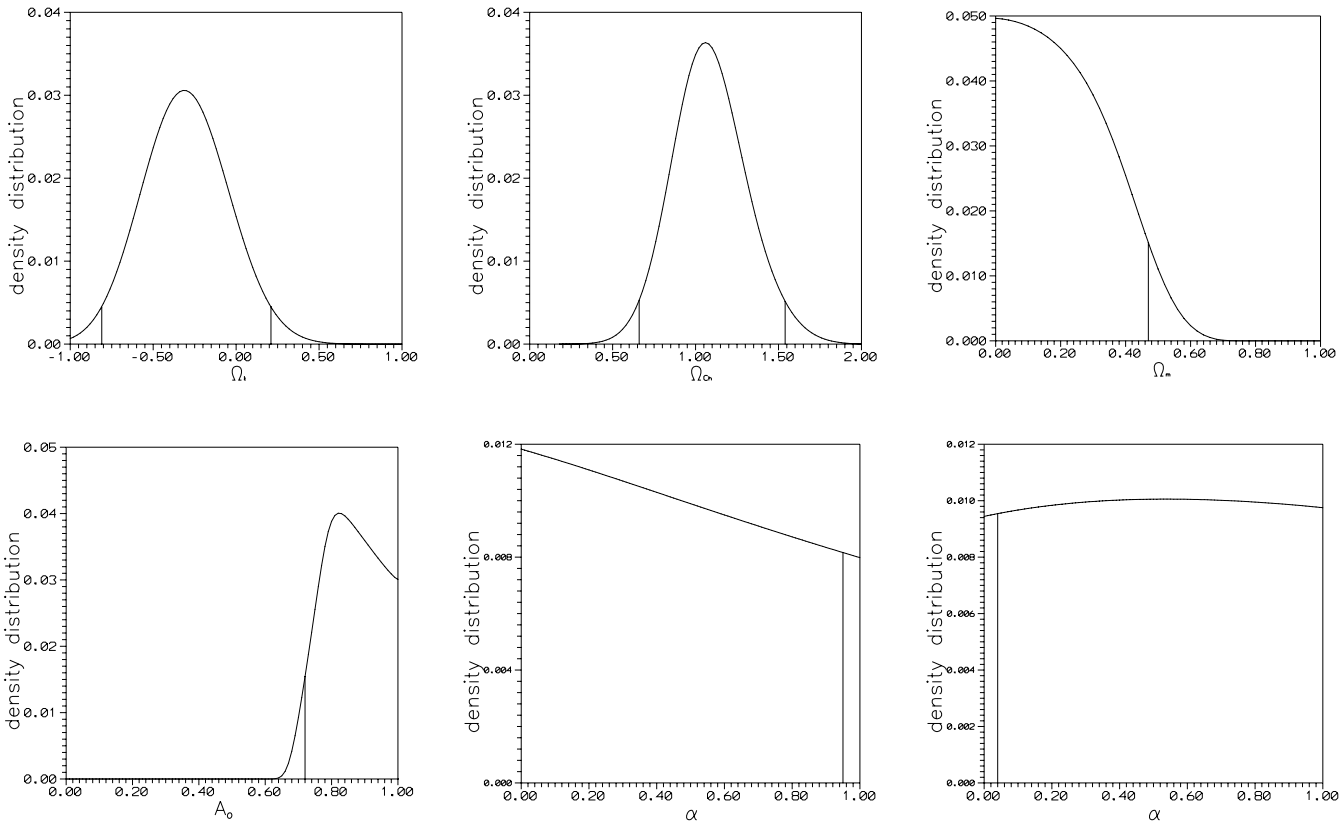


FIG. 4.—Density distributions (one-dimensional pdf's) for various cosmological parameters derived by marginalization over the remaining parameters of the model, from the Gold sample with the flat prior relaxed. We obtain the limits $\Omega_k \in (-0.81, 0.21)$, $\Omega_{\rm Ch} \in (0.66, 1.54)$, $\Omega_m \in (0, 0.47)$, $A_0 \in (0.72, 1)$, and $\alpha < 0.95$ at the confidence level of 95.4%. For comparison, we present (*bottom right panel*) the one-dimensional pdf for the α-parameter obtained from the baryonic model ($\Omega_m = 0.05$) Gold sample, where we obtained $\alpha > 0.04$ at the confidence level of 95.4%.

analyze Knop and Riess samples. One can see that estimation of other model parameters gives similar results for both samples, with the exception of parameter α. Specifically, for the toy and baryonic models the maximum-likelihood method prefers a universe with a nonzero parameter α, as for the flat universe case. One can see that when we analyze the Gold sample with the flat prior relaxed, the errors in the estimation of the model parameters significantly decrease (as compared with the case of the Knop sample).

4. GENERALIZED CHAPLYGIN GAS MODEL IN PERSPECTIVE OF *SNAP* DATA

In the near future the *SNAP* mission is expected to observe about 2000 SNe Ia each year, over a period of 3 yr.[1] Therefore, it could be possible to discriminate between various cosmological

[1] See http://www-supernova.lbl.gov and http://snfactory.lbl.gov.

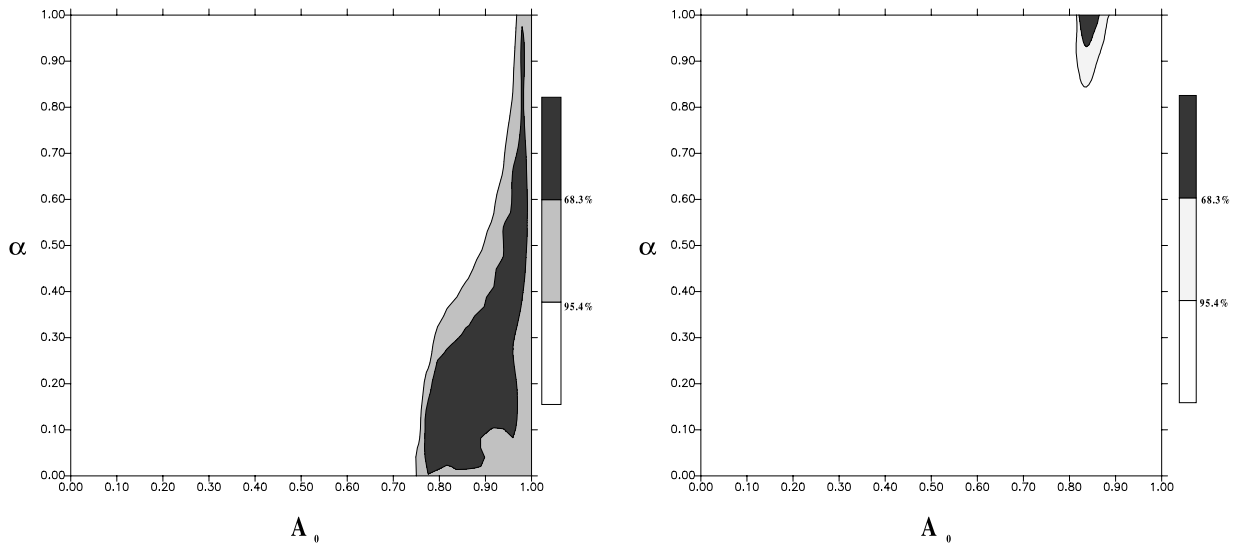


FIG. 5.—Confidence levels on the plane (A_0, α) for sample X1 (ΛCDM model; *left panel*) and X2 (Cardassian model; *right panel*) of simulated *SNAP* data, marginalized over Ω_m. The figure shows the ellipses of preferred values of A_0 and α.

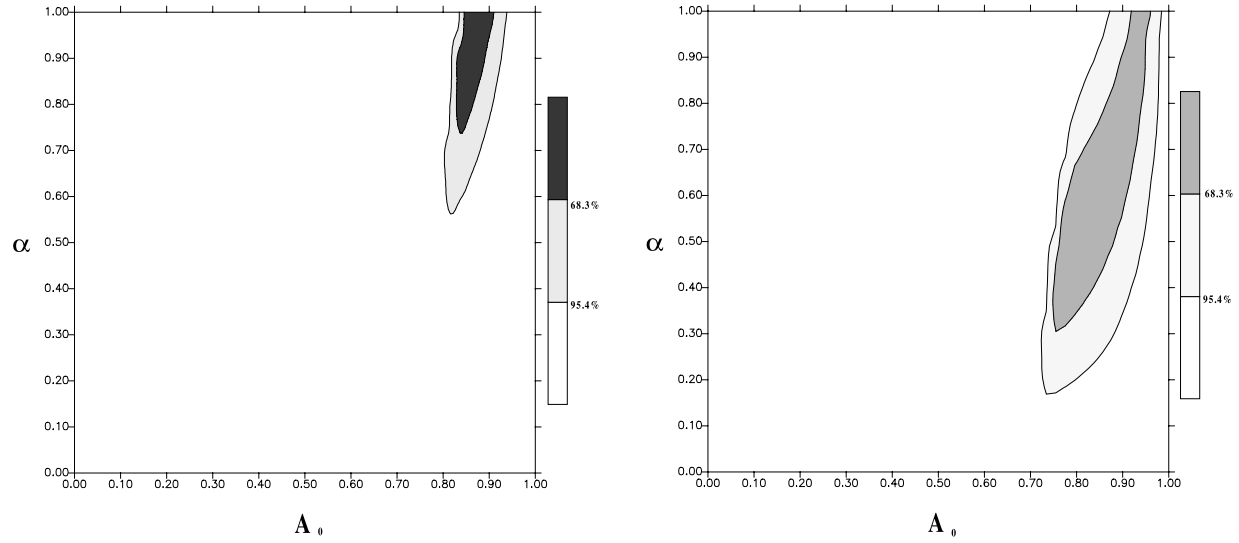


FIG. 6.—Confidence levels on the plane (A_0, α) for sample X3a (GCG model, $\Omega_m = 0$, $A_0 = 0.85$ and $\alpha = 1$; *left panel*) and sample X3b (GCG model, $\Omega_m = 0$, $A_0 = 0.76$ and $\alpha = 0.49$; *right panel*) of simulated *SNAP* data, marginalized over Ω_m. The figure shows the ellipses of preferred values of A_0 and α.

models, since errors in the estimation of model parameters would decrease significantly. We tested how a large number of new data would influence the errors in the estimation of model parameters. We assumed that the universe is flat and tested three classes of cosmological models. In the first, the ΛCDM model, we assumed $\Omega_m = 0.25$, $\Omega_\Lambda = 0.75$, and $\mathcal{M} = -3.39$ (Knop et al. 2003). The second class was representative of the so-called Cardassian models (Freese & Lewis 2002), with parameters $\Omega_m = 0.42$, $\Omega_{\rm Card} = 0.52$, and $n = -0.77$, as obtained in Godłowski et al. (2004). Let us note that at the level of the Hubble diagram test, Cardassian models are equivalent to quintessence models. The difference is in the underlying philosophy: quintessence assumes an exotic dark energy component with a hydrodynamic equation of state in the ordinary FRW model, while the Cardassian universe assumes a modification of the Friedman equation (which can be either due to an exotic matter component or due to modification of the gravity law). The last model was the GCG model with the parameters obtained in the present paper as best fits for the K3 sample ($\Omega_m = 0$, $A_0 = 0.85$ and $\alpha = 1$). These values are in agreement with results of the analysis performed on Tonry-Barris and Riess samples. Alternatively, we also test the GCG model with a small value of the α-parameter, suggested (from marginal pdf's) by analysis of the Perlmutter and Knop samples ($\Omega_m = 0$, $A_0 = 0.76$, and $\alpha = 0.40$). For the three above-mentioned models, we generated samples of 1915 supernovae (samples X1, X2, X3a, and X3b, respectively) in the redshift range $z \in [0.01, 1.7]$, distributed according to predicted *SNAP* data (see Table 1 of Alam et al. 2003). We assumed a Gaussian distribution of uncertainties in the measurement of m and z. The errors in redshifts z are of the order of 1 $\sigma = 0.002$, while the uncertainty in the measurement of magnitude m is assumed to be 1 $\sigma = 0.15$. The systematic uncertainty is $\sigma_{\rm sys} = 0.02$ mag at $z = 1.5$ (Alam et al. 2003). Hence one can assume that $\sigma_{\rm sys}(z) = (0.02/1.5)z$ as a first approximation. For such generated samples we repeated our analysis. The results of our analysis are presented in Figures 5 and 6. In these figures we present confidence levels on the plane (A_0, α) for samples of simulated *SNAP* data. The figures show the ellipses of preferred values of A_0 and α. It is easy to see that with the forthcoming *SNAP* data it will be possible to discriminate between the predictions of ΛCDM and GCG models. With the Cardassian model the situation is not so clear, however. Note that if $\alpha \simeq 0.4$, as suggested by analysis of Perlmutter sample C (see also Makler et al. 2003; Avelino et al. 2003; Fabris et al. 2002; Colistete et al. 2004), then it will be possible to discriminate between a model with Chaplygin gas and a Cardassian model (see Figs. 5 and 6). Moreover, it is clear that with the future *SNAP* data it will be possible to differentiate between models with various values of the α-parameter. This is especially valuable, since all analyses performed so far have had weak sensitivity with respect to α.

5. CONCLUSIONS

It is apparent that GCG models have brighter supernovae at redshifts $z > 1$. Indeed, one can see in Figures 2 and 3 (*left panels*) that the systematic deviation from the baseline Einstein–de Sitter model gets larger at higher redshifts. This prediction seems to be independent of the analyzed sample.

We found that the estimated value of A_0 is close to 0.8 in all considered models, with the exception of the class 1 model ($\Omega_m = 0.3$), when $A_0 > 0.95$. Relaxing the flat prior leads to the result that even though the best-fit values of Ω_k are formally nonzero, they are close to the flat case. This should be viewed as an advantage of the GCG model, since in similar analyses of the ΛCDM model in Riess et al. (1998) and Perlmutter et al. (1999) high negative values of Ω_k were found to be best fitted to the data, and independent inspiration from CMBR and extragalactic astronomy has been invoked to fix the curvature problem. Another advantage of the GCG model is that it leads in a natural way to the conclusion that the matter (baryonic) component should be small, which is in agreement with the BBN prediction. Estimates of A_0, Ω_k, and Ω_m are all independent of the sample used in our analysis.

Our results suggest that SN Ia data support the Chaplygin gas (i.e., $\alpha = 1$) scenario when the χ^2 best-fit procedure is used. The minimization procedure performed on Tonry-Barris and Riess data also gives $\alpha = 1$ (except for the model with fixed $\Omega_m = 0.3$). However, the maximum-likelihood fitting with the Knop et al. (2003) sample prefers, quite unexpectedly, a small value of α or even $\alpha = 0$, i.e., the ΛCDM scenario. Note that a small value of α is in agreement with the results obtained from CMBR (de Bernardis et al. 2000; Benoit et al. 2003; Hinshaw et al. 2003; Bento et al. 2002; Amendola et al. 2003) and with the recent analysis of Zhu (2004), who used combined data of

the X-ray gas mass fraction of the galaxy cluster, FR IIB radio galaxies, and the combined sample of Perlmutter et al. (1999) and Riess et al. (1998, 2001) to claim that α could even be less than zero. The results are dependent both on the sample chosen and on the prior knowledge of $\mathcal{M}$, in which the Hubble constant and intrinsic luminosity of SNe Ia are entangled. Moreover, the observed preference of A_0-values close to 1 means that the α dependence becomes insignificant (see eq. [8]). This is reflected in one-dimensional pdf's for α that turned out to be flat, meaning that the power of the present supernova data to discriminate between various GCG models (differing by α) is weak.

However, we argue that with future *SNAP* data it would be possible to differentiate between models with various values of the α-parameter. Residual plots indicate the differences between ΛCDM and GCG cosmologies at high redshifts. Therefore, one can expect that future supernova experiments (e.g., *SNAP*) having access to higher redshifts will eventually resolve the issue of whether the dark energy content of the universe could be described as a Chaplygin gas. The discriminative power of forthcoming *SNAP* data has been illustrated in Figures 5 and 6, obtained from the analysis on simulated *SNAP* data.

We thank B. J. Barris and A. G. Riess for explanation of the details of their SN Ia samples. M. S. was supported by KBN grant 2P03D00326. M. B. would like to express his gratitude to LJCh for continuous support.

REFERENCES

Alam, U., et al. 2003, MNRAS, 344, 1057
Alcaniz, J. S., Jain, D., & Dev, A. 2003, Phys. Rev. D, 67, 043514
Alcaniz, J. S., & Lima, J. A. S. 2005, ApJ, 618, 16
Amendola, L., Finelli, F., Burigana, C., & Carturan, D. 2003, J. Cosmol. Astropart. Phys., 07, 005
Avelino, P. P., Beça, L. M. G., de Carvalho, J. P. M., Martins, C. J. A. P., & Pinto, P. 2003, Phys. Rev. D, 67, 023511
Barris, B. J., et al. 2004, ApJ, 602, 571
Bean, R., & Doré, O. 2003, Phys. Rev. D, 68, 023515
Benoit, A., et al. 2003, A&A, 399, L25
Bento, M. C., Bertolami, O., & Sen, A. A. 2002, Phys. Rev. D, 66, 043507
———. 2003a, Phys. Rev. D, 67, 063003
———. 2003b, Phys. Lett. B, 575, 172
Bertolami, O., Sen, A. A., Sen, S., & Silva, P. T. 2004, MNRAS, 353, 329
Biesiada, M. 2003, Acta Phys. Polonica B, 34, 5423
Bilic, N., Lindebaum, R. J., Tupper, G. B., & Viollier, R. D. 2004, J. Cosmol. Astropart. Phys., 11, 008
Bordemann, M., & Hoppe, J. 1993, Phys. Lett. B, 317, 315
Caldwell, R. R., Dave, R., & Steinhardt, P. J. 1998, Phys. Rev. Lett., 80, 1582
Carturan, D., & Finelli, F. 2003, Phys. Rev. D, 68, 103501
Chaplygin, S. 1904, Sci. Mem. Moscow Univ. Math., 21, 1
Chiba, T., Sugiyama, N., & Nakamura, T. 1998, MNRAS, 301, 72
Choudhury, T. R., & Padmanabhan, T. 2005, A&A, 429, 807
Colistete, R., Fabris, J. C., Gonçalves, S. V. B., & de Souza, P. E. 2004, Int. J. Mod. Phys. D, 13, 669
Cunha, J. V., Lima, J. A. S., & Alcaniz, J. S. 2004, Phys. Rev. D, 69, 083501
de Bernardis, P., et al. 2000, Nature, 404, 955
Dev, A., Alcaniz, J. S., & Jain, D. 2003, Phys. Rev. D, 67, 023515
Fabris, J. C., Gonçalves, S. V. B., & de Souza, P. E. 2002, Gen. Relativ. Gravitation, 34, 2111
Freese, K., & Lewis, M. 2002, Phys. Lett. B, 540, 1
Frieman, J., Hill, C., Stebbins, A., & Waga, I. 1995, Phys. Rev. Lett., 75, 2077
Garousi, M. R. 2000, Nucl. Phys. B, 584, 284
Godłowski, W., Szydłowski, M., & Krawiec, A. 2004, ApJ, 605, 599
Gorini, V., Kamenshchik, A., & Moschella, V. 2003, Phys. Rev. D, 67, 063509
Hinshaw, G., et al. 2003, ApJS, 148, 135
Jackiw, R. 2000, A Particle Field Theorist's Lectures on Supersymmetric, Non-Abelian Fluid Mechanics and d-Branes (MIT-CTP 3000; Cambridge: MIT)
Kamenshchik, A., Moschella, V., & Pasquier, V. 2001, Phys. Lett. B, 511, 265
Knop, R. A., et al. 2003, ApJ, 598, 102
Kolda, C., & Lyth, D. 1999, Phys. Lett. B, 458, 197
Makler, M., de Oliveira, S. Q., & Waga, I. 2003, Phys. Lett. B, 555, 1
Maor, I., Brustein, R., & Steinhardt, P. J. 2001, Phys. Rev. Lett., 86, 6
Multamäki, T., Manera, M., & Gaztanaga, E. 2004, Phys. Rev. D, 69, 023004
Ogawa, N. 2000, Phys. Rev. D, 62, 085023
Peebles, P. J. E., & Ratra, B. 2003, Rev. Mod. Phys., 75, 559
Perlmutter, S., et al. 1999, ApJ, 517, 565
Randall, L., & Sundrum, R. 1999, Phys. Rev. Lett., 83, 4690
Ratra, B., & Peebles, P. J. E. 1988, Phys. Rev. D, 37, 3406
Riess, A. G., et al. 1998, AJ, 116, 1009
———. 2001, ApJ, 560, 49
———. 2004, ApJ, 607, 665
Sen, A. 2002, J. High Energy Phys., 04, 048
Silva, P. T., & Bertolami, O. 2003, ApJ, 599, 829
Szydłowski, M., & Czaja, W. 2004, Phys. Rev. D, 69, 023506
Tonry, J. L., et al. 2003, ApJ, 594, 1
Turner, M. S. 2002, ApJ, 576, L101
Turner, M. S., & White, M. 1997, Phys. Rev. D, 56, 4439
Weller, J., & Albrecht, A. 2001, Phys. Rev. Lett., 86, 1939
Williams, B. F., et al. 2003, AJ, 126, 2608
Zhu, Z. H. 2004, A&A, 423, 421